Neurochem Res (2017) 42:526–540
DOI 10.1007/s11064-016-2102-y

ORIGINAL PAPER

Altered Expression of CXCL13 and CXCR5 in Intractable Temporal Lobe Epilepsy Patients and Pilocarpine-Induced Epileptic Rats

Ruohan Li[1] · Limin Ma[1] · Hao Huang[1] · Shu Ou[1] · Jinxian Yuan[1] · Tao Xu[1] · Xinyuan Yu[1] · Xi Liu[1] · Juan Yang[1] · Yangmei Chen[1] · Xi Peng[1]

Received: 27 August 2016 / Revised: 13 October 2016 / Accepted: 7 November 2016 / Published online: 21 November 2016

Abstract The mechanisms that underlie the pathogenesis of epilepsy are still unclear. Recent studies have indicated that inflammatory processes occurring in the brain are involved in a common and crucial mechanism in epileptogenesis. C-X-C motif chemokine ligand 13 (CXCL13) and its only receptor, C-X-C motif chemokine receptor 5 (CXCR5), are highly expressed in the central nervous system (CNS) and participate in inflammatory responses. The present study aimed to assess the expression of CXCL13 and CXCR5 in the brain tissues of both patients with intractable epilepsy (IE) and a rat model (lithium-pilocarpine) of temporal lobe epilepsy (TLE) to identify possible roles of the CXCL13–CXCR5 signaling pathway in epileptogenesis. Real-time quantitative polymerase chain reaction (RT-qPCR), immunohistochemical, double-labeled immunofluorescence and Western blot analyses were performed in this study. CXCL13 and CXCR5 mRNA expression and protein levels were found to be significantly up-regulated in the TLE patients and TLE rats. Further, CXCL13 and CXCR5 protein levels were altered during the different epileptic phases after onset of status epilepticus (SE) in the pilocarpine model rats, including the acute phase (6, 24, and 72 h), latent phase (7 and 14 days) and chronic phase (30 and 60 days groups). Moreover, double-labeled immunofluorescence analysis revealed that CXCL13 was mainly expressed in the cytomembranes and cytoplasm of neurons and astrocytes, while CXCR5 was mainly expressed in the cytomembranes and cytoplasm of neurons. Thus, the CXCL13–CXCR5 signaling pathway may play a possible pathogenic role in IE. CXCL13 and CXCR5 may represent potential biomarkers of brain inflammation in epileptic patients.

Keywords CXCL13 · CXCR5 · Chemokines · Temporal lobe epilepsy · Inflammation · Pilocarpine

Introduction

Epilepsy is known as a chronic neurological disorder. It is one of the most common serious brain disorders. Current antiepileptic drugs (AEDs) suppress seizures without influencing the underlying tendency to generate seizures and are effective in 60–70% of epilepsy patients. Thus, 30–40% of epilepsy patients remain resistant to these drugs [1, 2]. Over the past 10 years, a plethora of evidence from clinical and experimental studies has revealed that brain inflammation plays an undeniable role in epileptogenesis. Normally, inflammatory cytokines are not expressed in brain tissue or are expressed at low levels. However, expression of these cytokines in brain tissue is increased in response to ischemia, trauma and excitotoxic brain damage [3]. The pathological process of chronic brain inflammation involves the activation of microglia, astrocytes and endothelial cells, disruption of the blood–brain barrier (BBB) and the production of inflammatory mediators. These changes also occur in epilepsy. Inflammation leads to destruction of the BBB and its increased permeability, the activation of gliacytes and the secretion of pro-inflammatory cytokines. These reactions further increase neuronal excitability and induce seizures. Inflammation also causes seizure recurrence and promotes resistance to common AEDs. A vicious

✉ Xi Peng
px5523@126.com

[1] Department of Neurology, Seond Affiliated Hospital of Chongqing Medical University, 74 Lin Jiang Road, Chongqing 400010, China

circle has been reported to occur between chronic brain inflammation and epilepsy [4].

Chemokines are cytokines are important mediators of leukocyte trafficking and the development of inflammation. Chemokines are able to target different subtypes of leukocytes to the inflammatory reaction zone and to induce chemotaxis of inflammatory cells within this zone. Studies of patients with epilepsy and animal models of temporal lobe epilepsy (TLE) have shown that chemokines and their receptors are involved in the pathophysiology of epilepsy [5]. Chemokines play a critical role in the migration of inflammatory cells to the central nervous system (CNS) through the BBB. Chemokine receptors are members of the seven transmembrane G protein-coupled receptor (GPCR) families. Recent studies have indicated that chemokines and their receptors are involved in immune-mediated CNS inflammation. Chemokines may induce neuronal death directly through activation of neuronal chemokine receptors, and chemokine receptors are also involved in neuronal death and hence in the development of neurodegenerative diseases [6, 7]. C-X-C motif chemokine ligand 13 (CXCL13), a cytokine belonging to the CXC chemokine family, also known as B lymphocyte chemoattractant (BLC) or B cell-attracting chemokine 1 (BCA-1), is a highly effective attractant for B lymphocytes and helper T cells that exerts its effects through C-X-C motif chemokine receptor 5 (CXCR5), also known as Burkitt's lymphoma receptor 1 (BLR1). CXCR5 is the only known ligand for this molecule, and it is highly expressed in B lymphocytes. CXCR5 plays a crucial role in lymphocyte trafficking within secondary lymphoid tissues [8–10]. Recent evidence has indicated that CXCL13 is expressed in the CNS and that it participates in inflammatory responses in many brain disorders, and it is considered the main factor promoting the increase in B lymphocytes in neuroinflammatory reactions. CXCL13 is involved in a variety of CNS inflammatory responses in immune-related diseases such as multiple sclerosis (MS), Lyme neuroborreliosis, primary CNS lymphoma (PCNSL), anti-*N*-methyl-D-aspartate receptor (NMDAR) encephalitis, HIV encephalopathy and neurosyphilis, and it may be a biomarker for these diseases [8].

Although CXCL13 is involved in a variety of CNS inflammatory diseases, this chemokine and its receptor, CXCR5, have not been assessed in studies of epilepsy to date. Based on the physiological roles of CXCL13 and CXCR5 in neuroinflammation and the roles of brain inflammation in epileptogenesis, it is important to determine whether they are involved in the pathogenesis of TLE. No study has assessed the expression of CXCL13 or CXCR5 in brain tissues of TLE patients or in TLE rat models. In this study, we measured the expression of CXCL13 and CXCR5 in the temporal neocortices of TLE patients and in the hippocampus and adjacent cortices of lithium chloride-pilocarpine-induced TLE model rats at different time points after onset of status epilepticus (SE) by real-time quantitative polymerase chain reaction (RT-qPCR), immunohistochemical, double-labeled immunofluorescence and Western blot analyses.

Experimental Procedures

Human Subjects

Twenty intractable TLE temporal neocortex samples and 20 histologically normal temporal neocortex samples were selected randomly from the Xinqiao Hospital of the Third Military University and the First Affiliated Hospital of Chongqing Medical University, China. All intractable TLE temporal neocortex samples were from patients with TLE who had the typical clinical manifestations and characteristic electroencephalogram (EEG) findings. The clinical features of the intractable TLE patients are shown in Table 1. Twenty histologically normal temporal neocortex samples were obtained from severe brain trauma patients who required surgery, did not experience seizures after the trauma, and did not have a prior history of epilepsy or any other neurologic disorder. The clinical features of the control patients are shown in Table 2.

Experimental Animals

Healthy adult male Sprague–Dawley rats (n = 64) weighing 180–240 g were obtained from the Experimental Animal Center of Chongqing Medical University, China. The experimental animals were randomly divided into a normal control group (n = 8) and TLE model group (n = 8 per subgroup). The TLE model group was randomly divided into the following seven subgroups: 6, 24, 72 h, 7, 14, 30, and 60 days after SE. Epilepsy modeling was carried out as reported previously [11]. The animals were maintained in a temperature-controlled room (27 °C) with a 12 h light/12 h dark cycle (lights on 6AM), and they were allowed free access to food and water. The rats in the TLE model group were administered intraperitoneal (i.p.) injection of lithium chloride (LiCl, 127 mg/kg, Sigma-Aldrich, St. Louis, MO, USA). Approximately 20 h later, atropine sulfate (1 mg/kg, i.p ; Sigma-Aldrich, USA) was administered to limit the peripheral effects of the convulsant. Pilocarpine (50 mg/kg, i.p.; Sigma-Aldrich, USA) was provided after 30 min. The rats then received repeated injections of pilocarpine (10 mg/kg, i.p.) every 30 min until they developed seizures. Seizures were scored in each rat using Racine's scale [12], and the rats at stage 4 or 5 were considered successfully kindled. At 1 h after the onset of SE, the rats were injected with diazepam (10 mg/kg, i.p.; Sigma-Aldrich, USA). The

Table 1 Clinical characteristics of the TLE patients

No.	Sex (M/F)	Age (years)	Duration (years)	AEDs	Resected tissue	Pathology result
1	M	7	3	OXC, CLB, VPA, TPM	LTN	G
2	F	12	5	OXC, VPA, GBP	LTN	G, NL
3	F	23	8	OXC, VPA, TPM	RTN	G, NL
4	F	17	5	VPA, CBZ, TPM	RTN	G, NL, ND
5	M	27	5	CBZ, VPA, CLB	LTN	G, NL, ND
6	M	13	7	LTG, TPM, CBZ	RTN	G
7	F	21	4	VPA, PB, CBZ, LEV	LTN	G, NL, ND
8	M	36	18	CBZ, VPA, CLB, TPM	LTN	G, NL, ND
9	M	16	7	OXC, VPA, PHT	LTN	G, NL
10	F	28	11	VPA, CBZ, PHT	RTN	G, NL
11	M	31	15	VPA, PB, CBZ, LEV	RTN	G, NL, ND
12	F	45	20	CBZ, PHT, VPA, PB	LTN	G, NL, ND
13	M	30	7	VPA, PB, CBZ	RTN	G, NL, ND
14	M	25	6	PHT, VPA, PB, TPM	LTN	G, NL, ND
15	M	33	12	CBZ, PHT, LTG	RTN	G, NL, ND
16	M	20	8	CBZ, PB, LTG, LEV	RTN	G, NL
17	M	15	9	LTG, TPM, CBZ	RTN	G, NL
18	F	21	4	VPA, CBZ, PB	LTN	G, NL
19	M	24	5	CBZ, PHT, PB, LTG	LTN	G, NL, ND
20	F	25	8	CBZ, PB, LTG, LEV	RTN	G, NL

F female, *M* male, *AEDs* anti-epileptic drugs, *OXC* oxcarbazepine, *CLB* clonazepam, *VPA* valproic acid, *TPM* topiramate *GBP* gabapentin, *CBZ* carbamazepine, *LTG* lamotrigine, *PB* phenobarbital, *LEV* levetiracetam, *PHT* phenytoin, *RTN* right temporal neocortex, *LTN* left temporal neocortex, *NL* neuronal loss, *ND* neuronal degeneration, *G* gliosis

Table 2 Clinical characteristics of the control group

No.	Sex (M/F)	Age (years)	Etiology diagnosis	Resected tissue	Seizure	Pathologic result
1	F	13	Brain trauma	LTN	None	Normal
2	M	24	Brain trauma	LTN	None	Normal
3	M	20	Brain trauma	RTN	None	Normal
4	M	25	Brain trauma	LTN	None	Normal
5	F	25	Brain trauma	RTN	None	Normal
6	M	31	Brain trauma	LTN	None	Normal
7	M	18	Brain trauma	LTN	None	Normal
8	M	44	Brain trauma	RTN	None	Normal
9	F	36	Brain trauma	LTN	None	Normal
10	F	33	Brain trauma	RTN	None	Normal
11	F	22	Brain trauma	RTN	None	Normal
12	M	16	Brain trauma	RTN	None	Normal
13	M	19	Brain trauma	RTN	None	Normal
14	F	27	Brain trauma	LTN	None	Normal
15	M	20	Brain trauma	LTN	None	Normal
16	F	15	Brain trauma	LTN	None	Normal
17	F	9	Brain trauma	RTN	None	Normal
18	M	32	Brain trauma	RTN	None	Normal
19	F	28	Brain trauma	LTN	None	Normal
20	M	22	Brain trauma	RTN	None	Normal

F female, *M* male, *RTN* right temporal neocortex, *LTN* left temporal neocortex

rats in the control group were i.p. injected with the same volume of physiological saline. Following the onset of SE, the model rats experienced an acute phase (6, 24, and 72 h), followed by a seizure-free period known as the latent phase (7 and 14 days) and then a chronic phase with spontaneous recurrent seizures (SRS, 30 and 60 days). The animals were sacrificed at various time points after SE, and the hippocampus and adjacent cortex were removed from each rat for analysis. The animal experimental procedures were performed according to the guidelines of the Ethical Committee and the Animal Care Committee of Chongqing Medical University, China. All efforts were made to minimize the number of animals used and their suffering.

Tissue Processing

Both the human temporal neocortex samples and rat brain tissues were divided into three portions. One portion was immediately stored in liquid nitrogen for Western blot and RT-qPCR analyses. Another portion was fixed in 4% paraformaldehyde for 24 h and then embedded in paraffin. All paraffin-embedded human and rat tissues were sectioned into 5 μm-thick paraffin slices, which were stored at 4 °C for subsequent use in immunohistochemical analyses. The other portion was fixed in 4% paraformaldehyde for 24 h, successively placed in 20 and 30% graded sucrose solution for 24 h (per solution), sliced into 10 μm-thick sections using a freezing microtome and then stored at −20 °C for double-labeled immunofluorescence analysis.

Real-Time Quantitative Polymerase Chain Reaction

Total RNA was extracted from the human temporal neocortex and rat hippocampus and adjacent cortex tissues using Trizol reagent (Takara, Japan), according to the manufacturer's instructions. RNA concentration and purity were assessed with a biophotometer (Thermo NanoDrop2000, USA). RNA samples with an A260/A280 ratio of between 1.8 and 2.0 were considered to be of sufficient quality for reverse transcription. The total RNA was reverse transcribed into complementary DNA (cDNA) with the Applied Biosystems Veriti®-Well Thermal Cycler (Thermo, USA) using a PrimeScript RT reagent Kit with gDNA Eraser (Takara, Japan). The reaction conditions for reverse transcription were 37 °C for 15 min and 85 °C for 5 s. Primers were designed and synthesized by Takara (Japan). GAPDH (human) and β-actin (rat) were used as internal control genes. The sequences and product sizes for each target gene are listed in Table 3. cDNA was amplified with an Eppendorf Realplex Real Time System (Eppendorf Mastercycle® ep realplex, Germany) using SYBR® Premix ExTaq™ II (Takara, Japan) according to the manufacturer's protocol. The thermal cycling conditions for RT-qPCR were as follows: initial denaturation for 30 s at 95 °C, followed by 40 cycles at 95 °C for 5 s and 60 °C for 34 s, one cycle at 95 °C for 15 s, and final melting curve analysis from 65.0 to 95.0 °C (0.5 °C increments for 5 s). After RT-qPCR, amplification was verified, the melting curves were assessed, and the relative gene expression levels were calculated using the comparative Ct method [13].

Double-Labeled Immunofluorescence

The frozen sections were immersed in acetone at 4 °C for 20 min. Next, they were washed with phosphate-buffered saline (PBS) three times (5 min per time) and permeabilized with 0.4% Triton X-100. Then, the sections were heated in a microwave oven for 15 min at 92–98 °C in sodium citrate buffer (0.01 M, pH 6.0) for antigen retrieval. They were subsequently washed with PBS and incubated in normal donkey serum (Tianjing TBD Biotechnology, China) for 60 min, followed by incubation at 4 °C overnight

Table 3 Target gene-specific primers used for the RT-qPCR

Target gene (species)	Primer sequence (5′–3′)	Product size (bp)
CXCL13 (*Homo sapiens*)	F:GCTTGAGGTGTAGATGTGTCC R:CCCACGGGGCAAGATTTGAA	83
CXCR5 (*Homo sapiens*)	F:CTGGGAACTGGACAGATTGGAC R:TCTCCGTGGAACTGCGTGTC	209
GAPDH (*Homo sapiens*)	F:CTTTGGTATCGTGGAAGGACTC R:GTAGAGGCAGGGATGATGTTCT	132
CXCL13 (*Rattus norvegicus*)	F:CCTTGCAAAAATCAGGCTTCC R:CACCTTAGGCTGGTAATGCGTC	74
CXCR5 (*Rattus norvegicus*)	F:CTATTTGCCTTGCCAGAACTCC R:CACGAGCATCGGTAGCAGGA	165
β-Actin (*Rattus norvegicus*)	F:ACGGTCAGGTCATCACTATCG R:GGCATAGAGGTCTTTACGGATG	155

F forward, *R* reverse

with a mixture of a primary polyclonal goat anti-CXCL13 antibody (1:50; Santa Cruz, CA, USA) and mouse anti-Neun antibody (1:20; Merck Millipore, Germany) or mouse anti-GFAP antibody (1:200; Cell Signaling Technology, Beverly, MA, USA), or a mixture of a polyclonal rabbit anti-CXCR5 antibody (1:50; Beijing Biosynthesis Biotechnology, China) and mouse anti-Neun antibody (1:20; Merck Millipore, Germany) or mouse anti-GFAP antibody (1:200; Cell Signaling Technology). On the next day, the sections were washed three times with PBS and then incubated with fluorescein isothiocyanate (FITC)-conjugated donkey anti-mouse IgG (1:100; Proteintech, Wuhan, China) and donkey anti-goat IgG-CFL 594 (1:100; Santa Cruz, CA, USA) or FITC-conjugated donkey anti-mouse IgG (1:100; Proteintech, Wuhan, China) and Alexa Flour 594-conjugated donkey anti-rabbit IgG (1:50; Proteintech, Wuhan, China) in the dark for 60 min at 37 °C. Then, the sections were incubated in 4, 6-diamidino-2-phenylindole (DAPI; Keygen Biotech, Nanjing, China) at 37 °C for 8 min. Next, they were washed with PBS and mounted with 50% glycerol/PBS. Laser scanning confocal microscopy (Leica Microsystems Heidelberg GmbH, Germany) with an Olympus IX70 inverted microscope (Tokyo, Japan) equipped with a Fluoview FVX confocal scan head (Leica Microsystems Heidelberg GmbH) was performed to examine fluorescence.

Immunohistochemistry

The paraffin sections were deparaffinized in xylene for 20 min and then rehydrated in graded ethanol (100, 95, 80, and 70%; 5 min for each grade). Rehydrated sections were incubated in H2O2 (3%, 20 min) to block endogenous peroxide activity. Then, the sections were heated in a microwave oven for 15 min at 92–98 °C in sodium citrate buffer (0.01 M, pH 6.0) for antigen retrieval. Non-specific binding was blocked by incubating the sections with 5% BSA (Boster Biological Technology, Wuhan, China) at 37 °C for 30 min. After blocking, the sections were incubated overnight at 4 °C with a primary polyclonal goat anti-CXCL13 antibody (1:50; Santa Cruz, CA, USA) or polyclonal rabbit anti-CXCR5 antibody (1:50; Beijing Biosynthesis Biotechnology, China). Next, after sufficient washing with PBS, the sections were incubated with a rabbit anti-goat secondary antibody (Boster Biological Technology, Wuhan, China) or goat anti-rabbit secondary antibody (Boster Biological Technology, Wuhan, China) for 30 min at 37 °C and washed as described above. The sections were then treated with avidin-biotin-peroxidase complex (Boster Biological Technology, Wuhan, China) at 37 °C for 20 min and subjected to further extensive washing with PBS. Immunoreactivity was visualized with 3, 3-diaminobenzidine (DAB; Boster Biological Technology, Wuhan, China). After the appearance of brown particles under the microscope, the sections were washed with distilled water to stop the reaction. Then, counterstaining was performed with Harris hematoxylin. Negative controls were obtained by application of PBS instead of the primary antibody. Finally, images were captured after the dehydration and transparent sealing of the sections. An Olympus BX51 automatic microscope (Osaka, Japan) was used to collect digital images. Cells with buffy staining of the cytoplasm or membrane were considered positive for CXCL13 and CXCR5. An average optical density (OD) value for each image was automatically calculated by the computer. CXCL13 and CXCR5 expression levels were quantitatively analyzed using Image-Pro Plus 6.0 software.

Western Blot Analysis

The human temporal neocortex, rat hippocampus and adjacent cortex tissues were homogenized. Total proteins were extracted from the homogenized brain tissues using a whole protein extraction kit (Beyotime, Haimen, China). The protein concentrations were determined using an enhanced BCA Protein Assay Kit (Beyotime, Haimen, China). Equal amounts (50–100 μg per lane) of protein were separated by SDS–PAGE (5% stacking gel, 60 V, 30 min; 10% separating gel, 120 V, 60 min, Bio-Rad Laboratories) and then electrotransferred to polyvinylidene fluoride (PVDF) membranes (pore size 0.22; Millipore Corp., MA, USA) at 250 mA for 50–70 min. Next, the membranes were incubated in 5% skim milk at room temperature for 60 min to block nonspecific binding and subsequently incubated with a primary polyclonal goat anti-CXCL13 antibody (1:500; Santa Cruz, CA, USA), primary polyclonal rabbit anti-CXCR5 antibody (1:200; Beijing Biosynthesis Biotechnology, China), or primary polyclonal rabbit anti-GAPDH antibody (1:3000; Hangzhou Goodhere Biotechnology, China) at 4 °C overnight. On the following day, the membranes were washed three times with Tween-20-Tris-buffered saline (TBST; 10 min per time), incubated with a horseradish peroxidase-conjugated rabbit anti-goat IgG antibody (1:3000; Proteintech, Wuhan, China) or horseradish peroxidase-conjugated goat anti-rabbit IgG antibody (1:3000; Proteintech, Wuhan, China) at room temperature for 60 min and washed with TBST three times (10 min per time). The protein bands were visualized using an enhanced chemiluminescence substrate kit (Beyotime Institute of Biotechnology, China) and digitally scanned (Vilber Lourmat Fusion Fx5, France). The ODs of the bands were quantified using ImageJ software. Then, the mean ODs of CXCL13 and CXCR5 were normalized to that of GAPDH.

Statistical Analysis

The results are expressed as the mean ± standard deviation (SD). There were eight groups of rat model, including control group and seven subgroups of pilocarpine-Induced TLE group, differences between TLE groups and control group of rat model were determined by one-way ANOVA analysis. Student's *t*-test was used for statistical analyses between the TLE group and the control group in human. P values of <0.05 were considered statistically significant. All statistical analyses were conducted using SPSS 22.0 statistical software.

Results

Demographic and Clinical Characteristics of the Human Subjects

The patients in the TLE group had a mean age of 23.35 ± 9.05 years and included 12 males and 8 females. The mean disease duration of these patients was 8.35 ± 4.68 years. The control group had a mean age of 23.95 ± 8.45 years and consisted of 11 males and 9 females. There was no significant difference in age or sex between the TLE and control groups (P > 0.05).

mRNA Expression of CXCL13 and CXCR5 in Intractable TLE Patients and TLE Rats

RT-qPCR was performed to detect the mRNA expression of CXCL13 and CXCR5 in the temporal neocortices of the TLE patients. The results revealed that these mRNA levels were up-regulated compared with the controls (P < 0.05) (Fig. 1a, b). In addition, their expression was up-regulated (P < 0.05) in the hippocampus of the TLE rats (30 and 60 days groups, in which the rats presented with SRS) and in the adjacent cortices of the TLE rats (Fig. 1c, d).

Localization of CXCL13 and CXCR5 in TLE Patients and Model Rats

Double-labeled immunofluorescence analysis was conducted to determine the cellular distribution of CXCL13 and CXCR5 in the temporal neocortices of the TLE patients and in the hippocampus and adjacent cortices of the pilocarpine model rats. The results revealed that the CXCL13

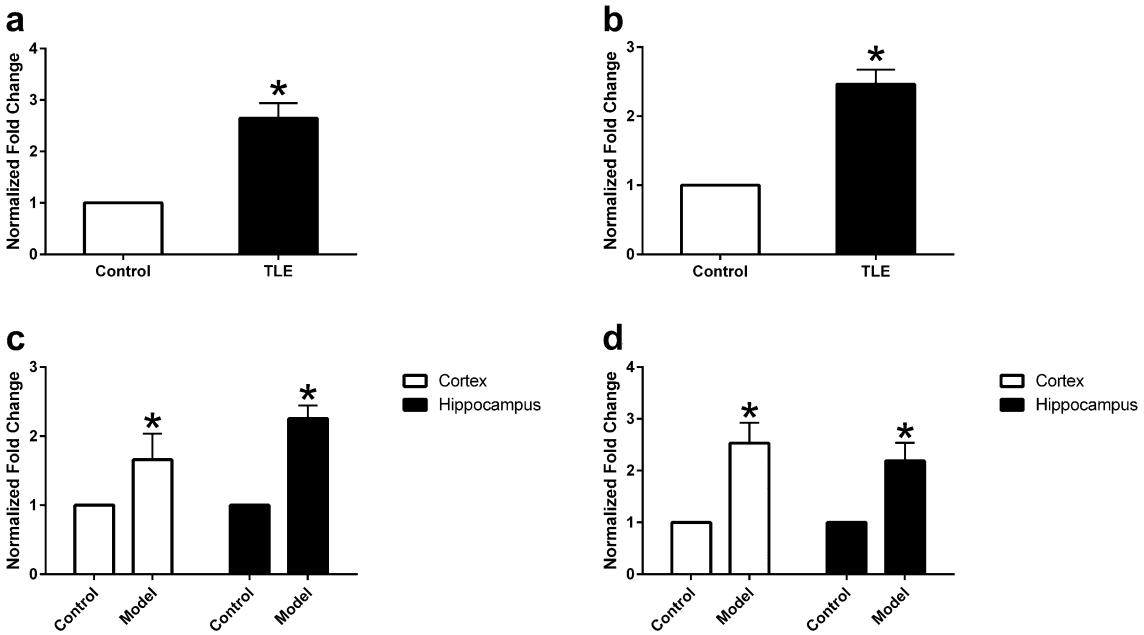

Fig. 1 The CXCL13 and CXCR5 mRNA levels were measured by RT-qPCR, and the changes in mRNA expression in the intractable TLE patients and TLE rats were expressed as fold changes relative to the expression in controls; GAPDH (human) and β-actin (rat) were used as internal control genes. The CXCL13 and CXCR5 mRNA levels were up-regulated in the temporal neocortices of the TLE patients and in the hippocampus and adjacent cortices of the TLE rats. **a** CXCL13 mRNA expression in the temporal neocortices of the intractable TLE patients. **b** CXCR5 mRNA expression in the temporal neocortices of the intractable TLE patients. **c** CXCL13 mRNA expression in the hippocampus and adjacent cortices of the TLE rats. **d** CXCR5 mRNA expression in the hippocampus and adjacent cortices of the TLE rats. *P < 0.05 versus control

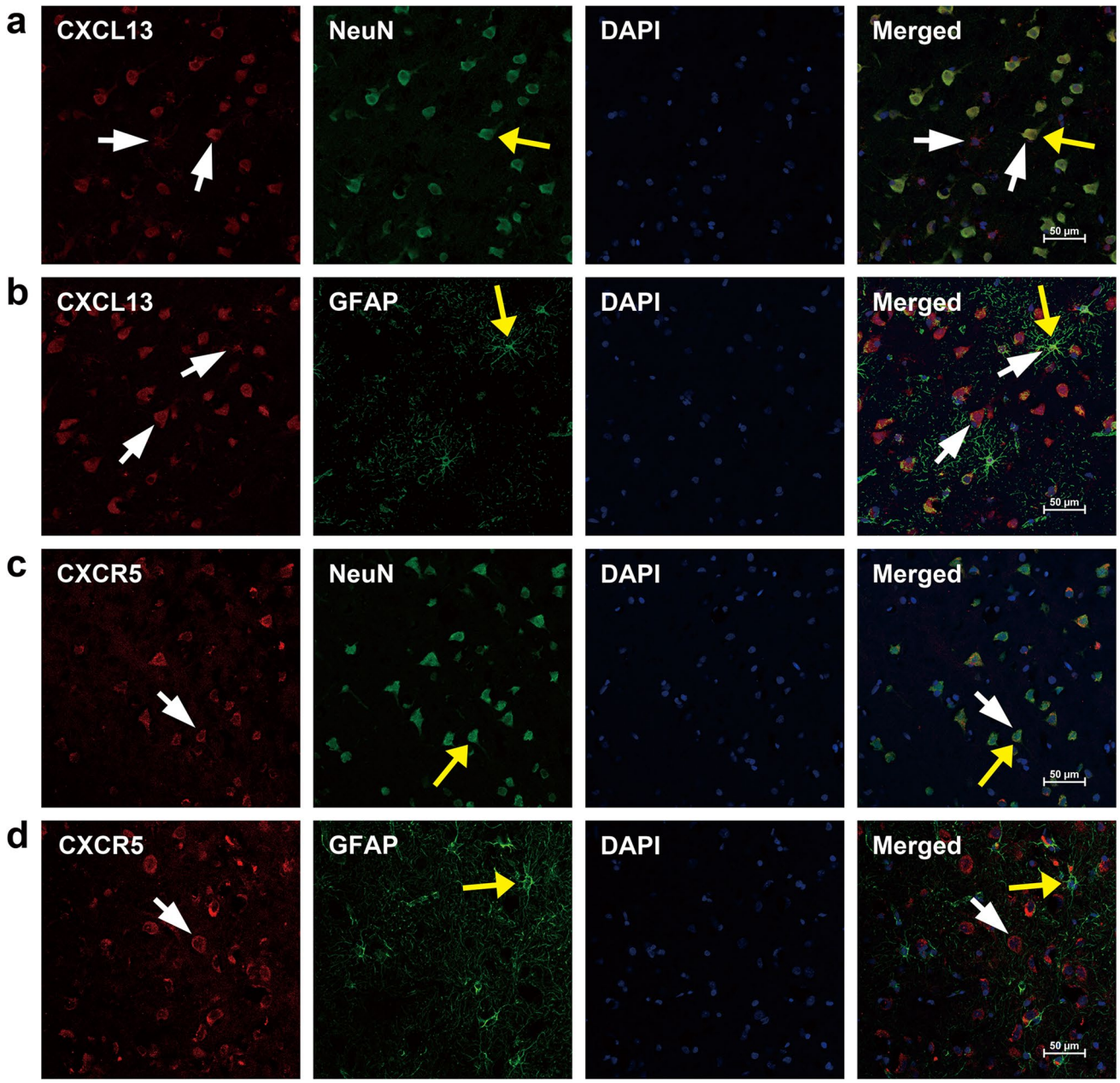

Fig. 2 Double-labeled immunofluorescence staining revealed the presence of CXCL13-positive and CXCR5-positive cells in the temporal neocortices of the intractable TLE patients. CXCL13 (*red*) was co-expressed with NeuN-positive neurons (*green*) and GFAP-positive astrocytes (*green*) but was not co-expressed with DAPI-positive nuclei (*blue*) in the temporal neocortices (**a, b**). CXCR5 (*red*) was co-expressed with NeuN-positive neurons (*green*) but was not co-expressed with GFAP-positive astrocytes (*green*) or DAPI-positive nuclei (*blue*) in the temporal neocortices (**c, d**). These results indicated that CXCL13 was simultaneously expressed in the cytomembranes and cytoplasm of neurons and astrocytes of the TLE patients and that CXCR5 was mainly expressed in the cytomembranes and cytoplasm of neurons. *White arrows*: CXCL13-positive and CXCR5-positive cells; *yellow arrows*: NeuN-positive and GFAP-positive cells. *Scale bar* 50 μm. (Color figure online)

protein was expressed in the cytomembranes and cytoplasm of neurons and astrocytes, as shown by co-expression with the mature neuron marker NeuN and the astrocyte marker GFAP in the temporal neocortices of the TLE patients (Fig. 2a, b) and in the brain tissues of the model rats (Fig. 3). However, the CXCR5 protein was expressed in the cytomembranes and cytoplasm and was only colocalized with NeuN, and not GFAP, in the temporal neocortices of the TLE patients (Fig. 2c, d) and in the brain tissues of the model rats (Fig. 4).

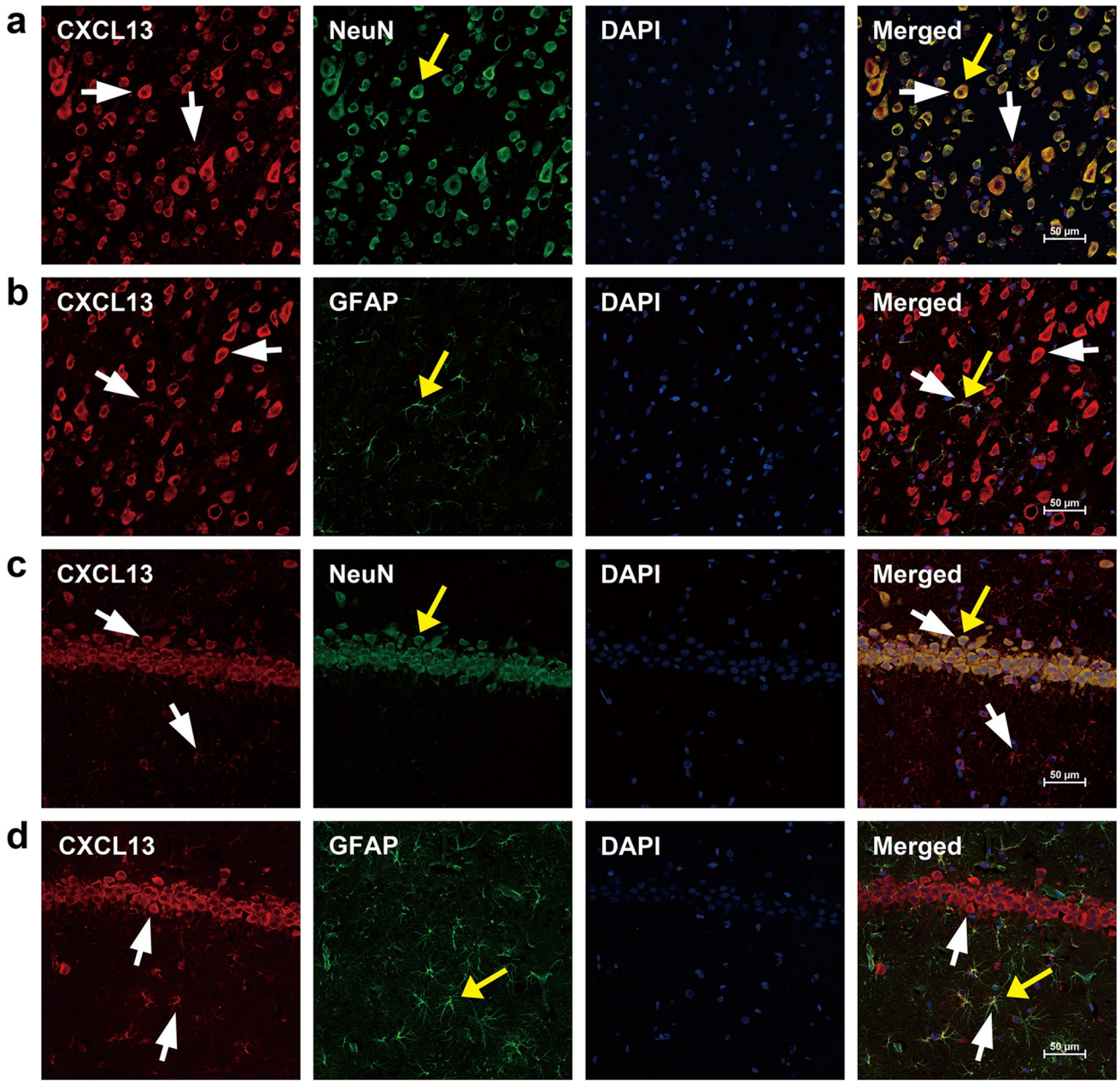

Fig. 3 Double-labeled immunofluorescence staining revealed the presence of CXCL13-positive cells in the hippocampus and adjacent cortices of the pilocarpine TLE model rats. CXCL13 (*red*) was co-expressed with NeuN-positive neurons (*green*) and GFAP-positive astrocytes (*green*) but not with DAPI-positive nuclei (*blue*) in the temporal neocortices (**a, b**) and in the hippocampal CA1 region (**c, d**). These results indicated that CXCL13 was simultaneously expressed in the cytomembranes and cytoplasm of neurons and astrocytes of the TLE model rats. *White arrows*: CXCL13-positive cells; *yellow arrows*: NeuN-positive and GFAP-positive cells. *Scale bar* 50 μm. (Color figure online)

Up-regulated CXCL13 and CXCR5 Expression in the Temporal Neocortices of the TLE Patients and in the Hippocampus and Adjacent Cortices of the Pilocarpine Model Rats

Immunohistochemical staining was performed to determine CXCL13 and CXCR5 expression in the brain tissues. The results showed that CXCL13 was primarily expressed in neurons and astrocytes. CXCL13 immunoreactivity was observed in the cytomembranes and cytoplasm of positive cells, and strong immunoreactivity for CXCL13 was detected in the positive cells in the temporal neocortices of the TLE patients and in the hippocampus and adjacent cortices of the TLE rats. In contrast,

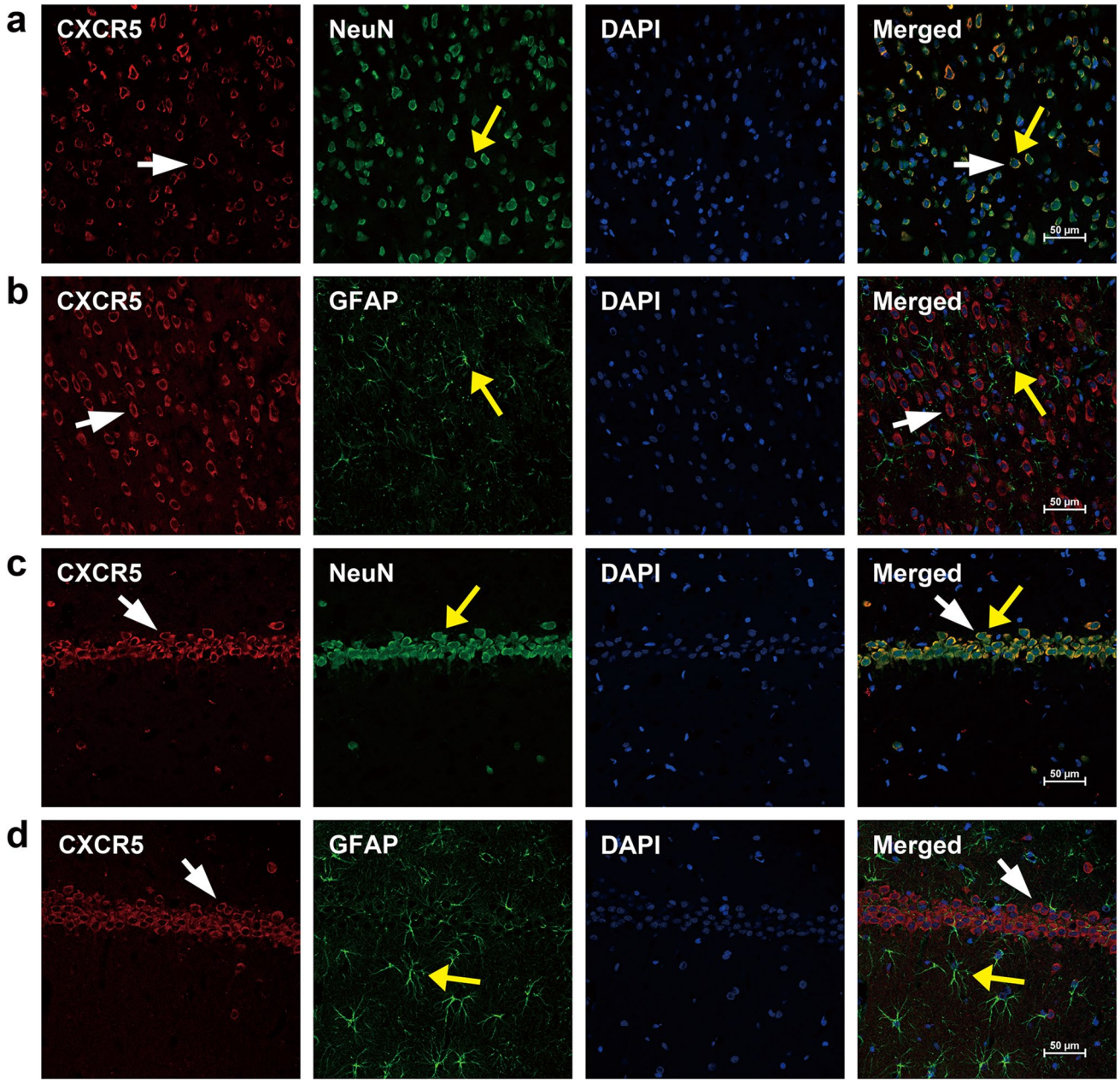

Fig. 4 Double-labeled immunofluorescence staining revealed the presence of CXCR5-positive cells in the hippocampus and adjacent cortices of the pilocarpine TLE model rats. CXCR5 (*red*) was co-expressed with NeuN-positive neurons (*green*) but not with GFAP-positive astrocytes (*green*) or DAPI-positive nuclei (*blue*) in the temporal neocortices (**a, b**) and in the hippocampal CA1 region (**c, d**). These results indicated that CXCR5 was mainly expressed in the cytomembranes and cytoplasm of neurons of the TLE model rats. *White arrows*: CXCR5-positive cells; *yellow arrows*: NeuN-positive and GFAP-positive cells. *Scale bar* 50 μm. (Color figure online)

faint immunoreactivity for CXCL13 was detected in the temporal neocortices of the human controls, as well as in the hippocampus and cortices of the rat controls. Statistical analysis revealed that the average OD of CXCL13 was significantly higher in the TLE patients and TLE rats than in the controls ($P < 0.05$) (Fig. 5). CXCR5 immunoreactivity was observed in the cytomembranes and cytoplasm of neurons, and up-regulated expression was detected in the brain tissues of the TLE patients and in the hippocampus and cortices of the TLE rats compared with that in the controls ($P < 0.05$) (Fig. 6). Additionally, the negative controls, in which the primary antibody was omitted, showed no immunoreactivity in neurons or glial cells.

Western blotting was performed to further verify the increased CXCL13 and CXCR5 immunostaining

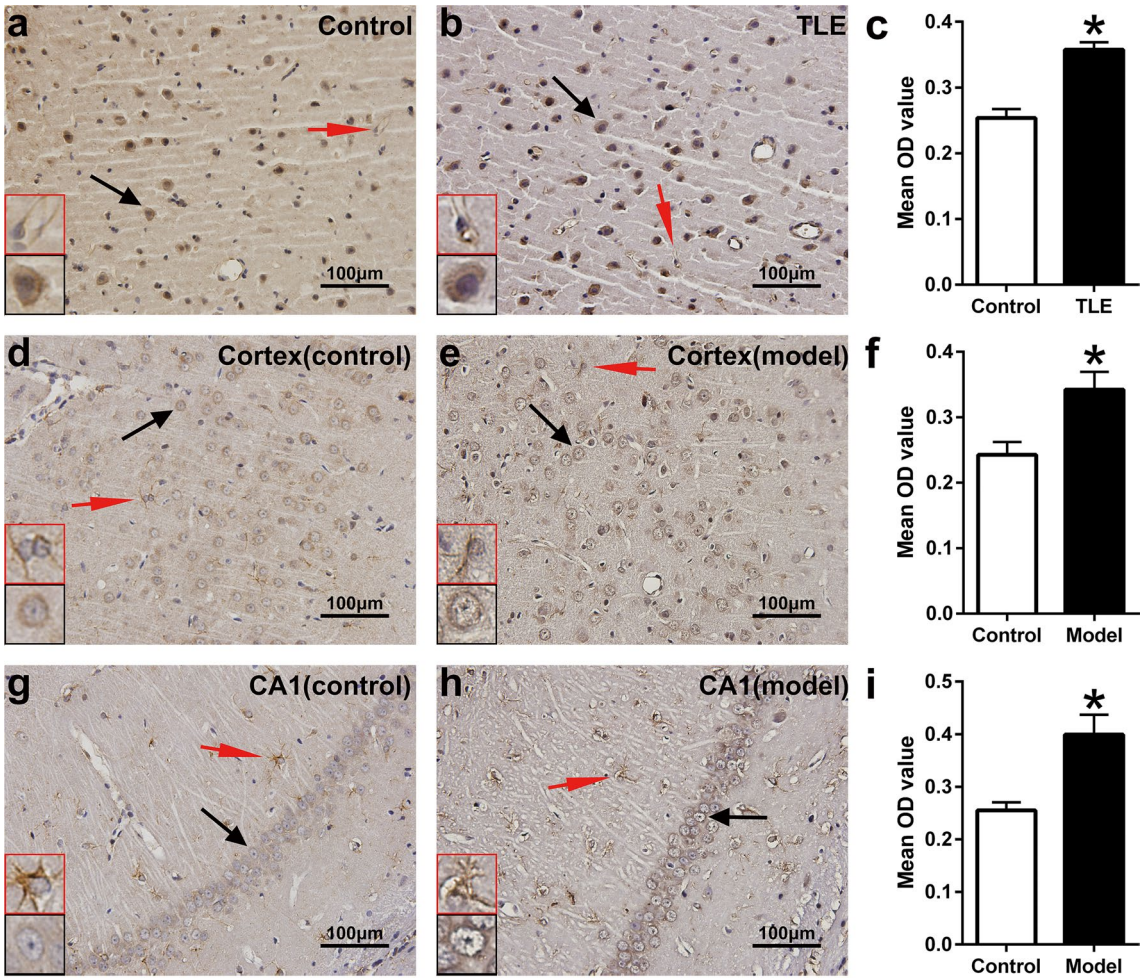

Fig. 5 CXCL13 expression was measured by immunohistochemistry. **a, b** CXCL13-positive cells in the temporal neocortices of the control and intractable TLE patients. **c** The bar graph shows that the average optical density of CXCL13-positive cells from the TLE patients was increased compared with that of the controls (n = 20 for each group). **d, e, g, h** CXCL13-positive cells in the temporal neocortices and hippocampal CA1 regions of the control and TLE rats. **f, i** The respective bar graph shows that the average optical density of CXCL13-positive cells was increased in the temporal neocortices and hippocampal CA1 region of the TLE rats compared with that of the controls (n = 5 for each group). *P < 0.05 versus control. The *red* and *black arrows* indicate the two different morphologies of the CXCL13-positive cells. *Scale bar* 100 μm. (Color figure online)

in the brains of the model rats. A CXCL13 immunoreactive band was observed at approximately 21 kDa, a CXCR5 immunoreactive band was detected at 50 kDa, and a GAPDH immunoreactive band was observed at approximately 37 kDa. CXCL13 and CXCR5 expression was normalized by calculating the intensity ratios of the bands relative to the GAPDH band. The results revealed that the CXCL13 and CXCR5 protein levels were significantly increased in the temporal neocortices of the intractable TLE patients compared with those in the controls ($P < 0.05$) (Fig. 7a–c). In the temporal neocortices of the model rats, the CXCL13 protein level was altered between the different groups ($F(7, 24) = 19.743$, $P = 0.000$) and was increased at 24 h, 30 and 60 days after SE compared with that in the controls ($P < 0.05$). In addition, the CXCR5 protein level was altered between the eight groups ($F(7, 24) = 14.447$, $P = 0.000$) and was increased from 24 h to 60 days compared with that in the controls ($P < 0.05$). This increasing trend was the most pronounced at 24 h after SE (Fig. 7d–f). In the hippocampus of the model rats, the CXCL13 ($F(7, 24) = 5.419$, $P = 0.001$) and CXCR5 ($F(7, 24) = 14.538$, $P = 0.000$) protein levels were altered between the different groups. The CXCL13 protein level did not change from 6 h to 7 days after SE. However, it gradually increased from 14 to 60 days after SE compared with that in the controls ($P < 0.05$), and significant increases in this level were observed at 14 and 60 days after SE. Further, the CXCR5 protein level was up-regulated from 6 h to 60 days after

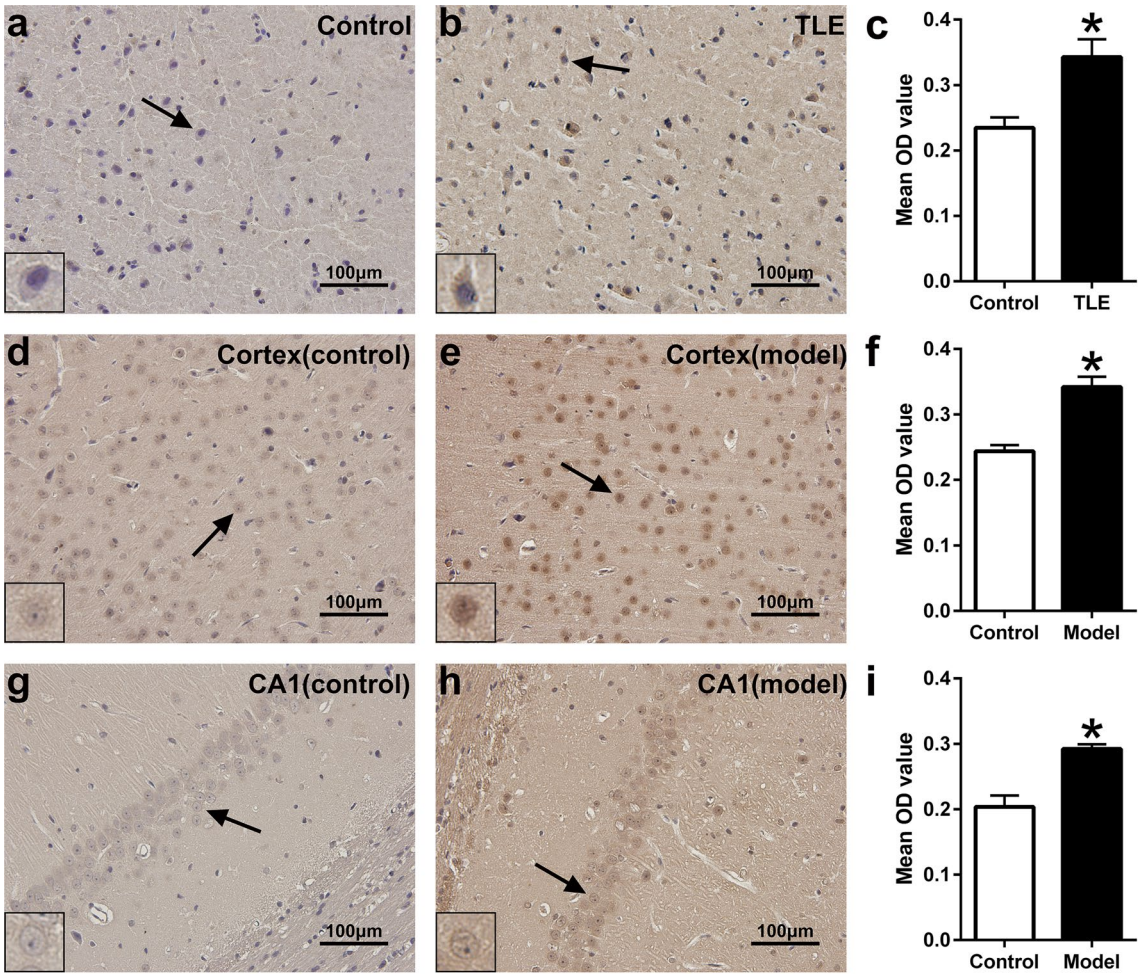

Fig. 6 CXCR5 expression was measured by immunohistochemistry. **a, b** CXCR5-positive neurons in the temporal neocortices of the control and intractable TLE patients. **c** The bar graph shows that the average optical density of CXCR5-positive cells was increased in the TLE patients compared with the controls. **d, e, g, h** CXCR5-positive cells in the temporal neocortices and hippocampal CA1 regions of the control and TLE rats. **f, i** The respective *bar graph* shows that the average optical density of the CXCR5-positive cells was increased in the temporal neocortices and hippocampal CA1 regions of the TLE rats compared with that of the controls. *$P < 0.05$ versus control. The *black arrows* indicate CXCR5-positive neurons. Scale bar 100 μm

SE, especially at 6 h, compared with that in the controls ($P < 0.05$) (Fig. 7g–i).

Discussion

Epileptogenesis is thought to occur in three stages: an initial insult or precipitating event; a latent period, which is a seizure-free period that can last from weeks to months and is characterized by cellular and molecular changes; and a chronic epilepsy phase, in which SRS occur [14]. In this study, we examined changes in CXCL13 and CXCR5 expression in the hippocampus and adjacent cortices of TLE model rats during the different epileptic phases, including the acute damage phase, latent phase and chronic phase, because only the chronic phase of TLE can be studied using human tissues.

Five major findings were initially obtained in this study. First, CXCL13 was found to be mainly expressed in neurons and astrocytes in the brains of the TLE patients and pilocarpine TLE model rats. CXCR5 was mainly expressed in neurons, but not in glial cells, in the brain tissues of the TLE patients and pilocarpine TLE model rats. Second, CXCL13 and CXCR5 mRNA expression was up-regulated in the temporal neocortices of the TLE patients and in the hippocampus and adjacent cortices of the TLE rats. Third, immunohistochemical rasults indicated that CXCL13 and CXCR5 expression was up-regulated in the brains of the intractable TLE patients and TLE rats. Fourth, the CXCL13 and CXCR5 protein levels were up-regulated in

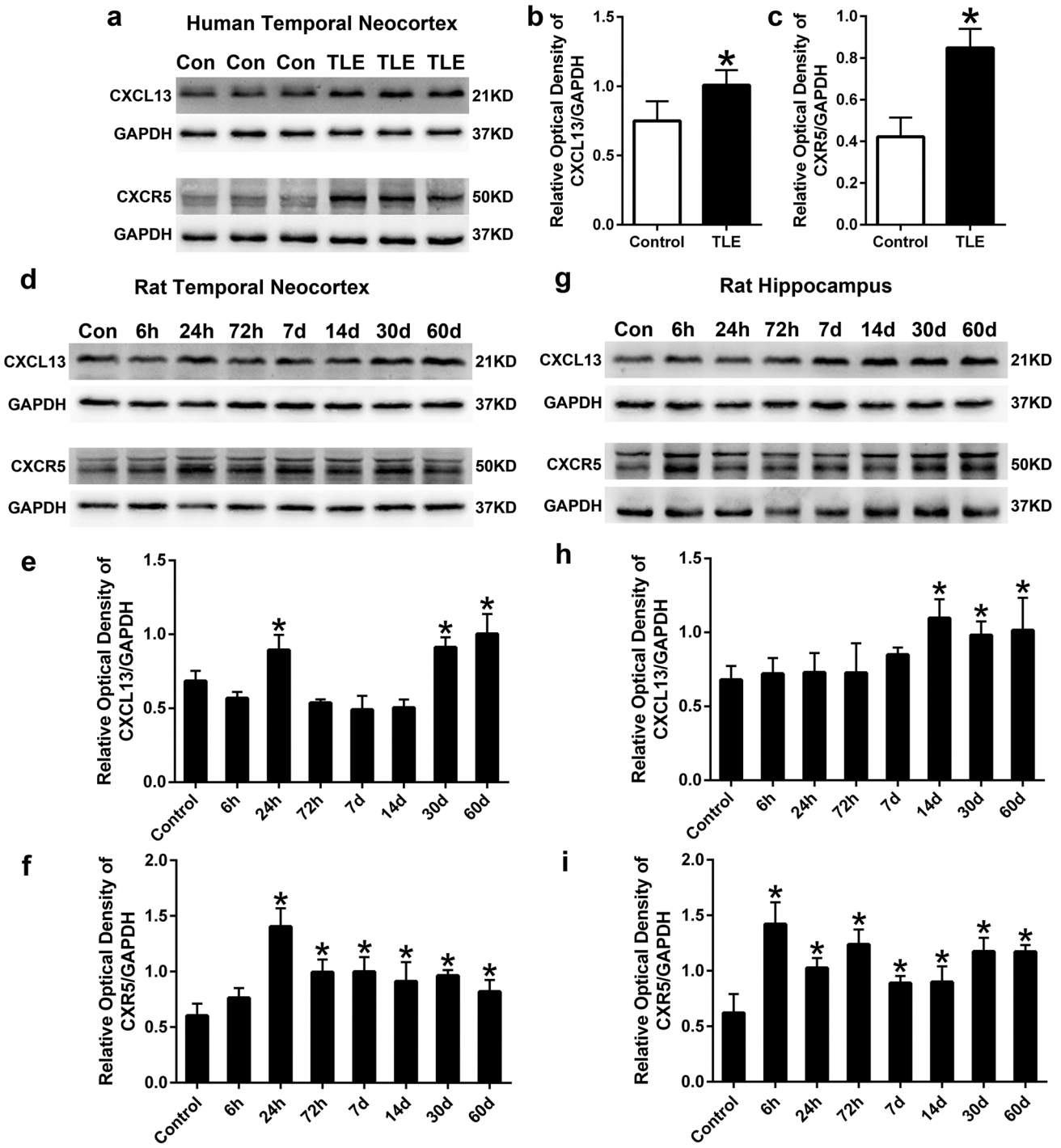

Fig. 7 CXCL13 and CXCR5 protein levels were detected by Western blot analysis. The relative optical densities of the CXCL13 and CXCR5 protein bands were normalized to that of the GAPDH band. **a** CXCL13 and CXCR5 protein expression in the temporal neocortices of the control and intractable TLE patients. **b, c** The respective *bar graph* shows that the CXCL13 and CXCR5 protein levels were up-regulated in the TLE patients compared with the controls. **d, g** CXCL13 and CXCR5 protein expression in the hippocampus and adjacent cortices of the control and TLE model rats. *Lane 1* shows CXCL13 or CXCR5 expression in the controls, and lane 2–8 depicts CXCL13 or CXCR5 expression in the hippocampus and adjacent cortices of the model rats at different time points after SE. **e, f, h, i** The respective *bar graph* shows that the CXCL13 and CXCR5 protein levels were altered at different time points after SE in the TLE model rats compared with the controls. *$P < 0.05$ versus control

TLE patients and at 30 and 60 days, chronic phase of TLE with SRS, in the hippocampus and temporal neocortices of the model rats. This finding is in agreement with the results of immunohistochemical and RT-qPCR. The finding of significant increases in the CXCL13 and CXCR5 mRNA and expression in the brain tissues of the TLE patients and TLE rats may suggest that this signaling pathway plays a pathogenic role in epileptogenesis. Finally, the CXCL13 and CXCR5 protein levels were obviously up-regulated at 24 h after onset of SE in the temporal neocortices of the pilocarpine-induced model rats. In the hippocampus of the model rats, the CXCL13 protein level exhibited a gradual increase from 14 to 60 days after SE. In addition, the CXCR5 level increased from 6 h to 60 days, especially at 6 h. These results indicated that inflammation may have occurred after acute damage of the brain tissues during seizures and that this inflammation may have induced the increases in the CXCL13 and CXCR5 levels; CXCL13 and CXCR5 expression was up-regulated from the latent phase to the chronic phase in the hippocampus and adjacent cortices of the model rats. Their increased expression during the latent phase may have induced SRS during the chronic phase. The exact pathophysiological mechanism requires further study in future drug testing and intervention experiments. In addition, the finding of alterations in the CXCL13 and CXCR5 protein levels at different time points after SE will aid in the selection of optimal intervention times.

Approximately 30% of individuals with epilepsy eventually develop intractable epilepsy (IE). This condition seriously affects the quality of life of TLE patients and increases the economic burden on patients' families. Evidence in the literature suggests that neuroinflammation is involved in the pathophysiology of IE. Studies of epileptic animal models have demonstrated that seizure activity can induce neuroinflammation and that chronic inflammation is maintained by recurrent seizures [15]. Inflammation may be an etiology of epilepsy, and it can also result from epileptic seizures. Inflammation can repeatedly prolong the disease course, promote the development of resistance to conventional AEDs and induce the development of drug-resistant epilepsy. Inflammation is not an accidental symptom in the pathological process of epilepsy. Knowledge of these inflammatory mechanisms may facilitate the identification of novel drug targets that can both control the symptoms of and prevent the formation of drug-resistant epilepsy.

Although the mechanisms of epileptogenesis are still unknown, pro-inflammatory cytokines may play a critical role in the pathogenesis of epilepsy [16]. Various experimental and clinical evidence suggests that inflammation plays a common and important role in the pathogenesis of human epilepsy. In a study of kainic acid (KA)-induced epileptic rats, Vezzani et al. have found that the expression of various pro-inflammatory cytokines and autoimmune markers, such as nuclear factor-kappa B (NF-κB), cyclooxygenase-2 (COX-2), Toll-like receptor family members, monocyte chemoattractant protein and various complement components, is up-regulated in neurons and glial cells [17]. Voutsions-Porche et al. have found that NF-κB, COX-2, and interleukin-1 beta (IL1-B) expression was also up-regulated in the hippocampus of the lithium-pilocarpine TLE model rats. Moreover, the damage to brain tissue caused by these inflammatory cytokines is closely associated with the duration of epileptic seizures [18]. In the hippocampus of KA-induced SE model rats during different developmental periods, neuronal injury has been reported to occur only when inflammatory cytokine expression is up-regulated. This characteristic of inflammatory cytokines in epilepsy differs from what is observed in inflammation of brain tissue caused by infection [19].

It is known that chemokines and chemokine receptors participate in a regulatory network characterized by and involved in the regulation of diversity in leukocyte recruitment [7]. In animal models of epilepsy, leukocyte trafficking mechanisms have been shown to induce BBB damage, leading to seizures [20]. Furthermore, chemokines modulate neuronal activity by: (a) modulating voltage-dependent channels (sodium, potassium, and Ca^{2+}); (b) activating the G-protein-activated inward rectifier potassium current; and (c) increasing neurotransmitter release (gamma-amino butyric acid (GABA), glutamate, and dopamine), often through Ca^{2+}-dependent mechanisms [21, 22]. CXCL13 is critical for B lymphocyte recruitment, and the CXCL13 protein level is often elevated in the inflamed CNS. Intrathecal accumulation of B lymphocytes and immunoglobulins is a prominent feature of many infectious and inflammatory disorders of the CNS [23]. CXCL13 plays a key role in the migration of B lymphocytes into the cerebrospinal fluid (CSF) through the BBB. A significant elevation in the CSF CXCL13 level has been reported in patients with CNS inflammatory diseases, such as MS, Lyme neuroborreliosis, neurosyphilis and anti-NMDAR encephalitis [24–27]. In addition, Legler et al. have assessed the activity of CXCL13 in transfected human blood B lymphocytes and have found that CXCL13 induces chemotaxis and Ca^{2+} mobilization via CXCR5 [9]. In our study, CXCL13 was found to be expressed in neurons and astrocytes and CXCR5 was mainly detected in neurons in the brains of the TLE patients and pilocarpine TLE model rats. Therefore, we suggest that after the CXCL13 protein binds to its receptor, CXCR5, in neurons, these molecules may mobilize Ca^{2+}, thereby enhancing GABA release. Kowarik M et al. have measured the concentrations of chemokines/cytokines in CSF and sera of patients with immune-related diseases of the CNS, such as clinically isolated syndrome (CIS), MS, Lyme neuroborreliosis and other inflammatory

neurological diseases. They found that only CXCL13 was significantly elevated in the CSF of all patients with the above-mentioned neuroinflammatory diseases. CXCL13, which recruits B cells to the CNS compartment, seems to be the major indicator of chronic immune inflammation in the CNS [28]. Our study revealed that CXCL13 mRNA and protein expression was up-regulated in the TLE patients and TLE rats compared with that in the controls. These findings indicate that CXCL13 may be involved in epileptogenesis. In addition, they suggest that chronic inflammation plays an important role in the pathological process of epilepsy. In research of mammalian hippocampal neurobiology, CXCR5 has been demonstrated to impair the maintenance of hippocampal neuroblasts and neuronal precursor cell populations. CXCR5 may have a detrimental effect on the hippocampal neuroblast precursor cell populations through an inflammatory or pro-apoptotic mechanism [29, 30]. Our study revealed that the CXCR5 protein level was up-regulated in the TLE patients and TLE rats, especially in the epileptic model rats with no SRS. These results demonstrate that CXCR5 may play a crucial role in epileptogenesis by inducing nerve apoptosis.

In conclusion, to the best of our knowledge, our study is the first report of abnormal CXCL13 and CXCR5 expression in intractable TLE patients and lithium-pilocarpine epilepsy model rats. The results of this study indicate that the up-regulation of CXCL13 and CXCR5 expression may contribute to the pathogenesis of epilepsy by promoting inflammation and mobilizing Ca^{2+}, thereby enhancing GABA release and inducing nerve apoptosis. Thus, CXCL13 and CXCR5 may serve as potential biomarkers for predicting TLE. However, the exact pathophysiological mechanism of the CXCL13–CXCR5 signaling pathway in epileptogenesis remains unclear, and further studies should be conducted in the future.

Acknowledgements This work was supported by the Young Scientists Fund of the National Natural Science Foundation of China (No. 81401073). We thank the patients and their families for their participation in this study. We also sincerely thank the Xinqiao Hospital of The Third Military Medical University and the First Affiliated Hospital of Chongqing Medical University for supplying the brain tissues used in this study.

Compliance with Ethical Standards

Conflict of interest The authors declare that they have no competing interests.

References

1. Amhaoul H, Staelens S, Dedeurwaerdere S (2014) Imaging brain inflammation in epilepsy. Neuroscience 279:238–252. doi:10.1016/j.neuroscience.2014.08.044
2. Duncan JS, Sander JW, Sisodiya SM, Walker MC (2006) Adult Epilepsy. The Lancet 367:1087–1100. doi:10.1016/S0140-6736(06)68477-8
3. Vezzani A, Friedman A, Dingledine RJ (2013) The role of inflammation in epileptogenesis. Neuropharmacology 69:16–24. doi:10.1016/j.neuropharm.2012.04.004
4. Vezzani A, French J, Bartfai T, Baram TZ (2011) The role of inflammation in epilepsy. Nat. Rev Neurol 7:31–40. doi:10.1038/nrneurol.2010.178
5. Kan AA, de Jager W, de Wit M, Heijnen C, van Zuiden M, Ferrier C, van Rijen P, Gosselaar P, Hessel E, van Nieuwenhuizen O, de Graan PN (2012) Protein expression profiling of inflammatory mediators in human temporal lobe epilepsy reveals co-activation of multiple chemokines and cytokines. J Neuroinflammation 9:207. doi:10.1186/1742-2094-9-207
6. Cartier L, Hartley O, Dubois-Dauphin M, Krause KH (2005) Chemokine receptors in the central nervous system: role in brain inflammation and neurodegenerative diseases. Brain Res Rev 48:16–42. doi:10.1016/j.brainresrev.2004.07.021
7. Glabinski A, Jalosinski M, Ransohoff RM (2005) Chemokines and chemokine receptors in inflammation of the CNS. Expert Rev Clin Immunol 1:293–301. doi:10.1586/1744666X.1.2.293
8. Huber AK, Irani DN (2015) Targeting CXCL13 during Neuroinflammation. Adv Neuroimmune Biol 6:1–8.
9. Legler DF, Loetscher M, Roos RS, Clark-Lewis I, Baggiolini M, Moser B (1998) B cell-attracting chemokine 1, a human CXC chemokine expressed in lymphoid tissues, selectively attracts B lymphocytes via BLR1/CXCR5. J Exp Med 187:655–660. doi:10.1084/jem.187.4.655
10. Moser B, Schaerli P, Loetscher P (2002) CXCR5(+) T cells: follicular homing takes center stage in T-helper-cell responses. Trends Immunol 23:250–254. doi:10.1016/S1471-4906(02)02218-4
11. Curia G, Longo D, Biagini G, Jones RS, Avoli M (2008) The pilocarpine model of temporal lobe epilepsy. J Neurosci Methods 172:143–157. doi:10.1016/j.jneumeth.2008.04.019
12. Racine R, Rose PA, Burnham WM (1977) Afterdischarge thresholds and kindling rates in dorsal and ventral hippocampus and dentate gyrus. Can J Neurol Sci 4:273–278. doi:10.1017/S0317167100025117
13. Schmittgen TD, Livak KJ (2008) Analyzing real-time PCR data by the comparative C(T) method. Nat Protoc 3:1101–1108. doi:10.1038/nprot.2008.73
14. Maguire J (2016) Epileptogenesis: more than just the latent period. Epilepsy Curr 16:31–33. doi:10.5698/1535-7597-16.1.31.
15. Vitaliti G, Pavone P, Mahmood F, Nunnari G, Falsaperla R (2014) Targeting inflammation as a therapeutic strategy for drug-resistant epilepsies: an update of new immune-modulating approaches. Hum Vaccin Immunother 10:868–875. doi:10.4161/hv.28400.
16. Fabene PF, Bramanti P, Constantin G (2010) The emerging role for chemokines in epilepsy. J Neuroimmunol 224:22–27. doi:10.1016/j.jneuroim.2010.05.016
17. Vezzani A, Balosso S, Ravizza T (2012) Inflammation and epilepsy. Handb Clin Neurol 107:163–175
18. Voutsinos-Porche B, Koning E, Kaplan H, Ferrandon A, Guenounou M, Nehlig A, Motte J (2004) Temporal patterns of the cerebral inflammatory response in the rat lithium-pilocarpine model of temporal lobe epilepsy. Neurobiol Dis 17:385–402. doi:10.1016/j.nbd.2004.07.023
19. Ravizza T, Rizzi M, Perego C, Richichi C, Velísková J, Moshé SL, De Simoni MG, Vezzani A (2005) Inflammatory response and glia activation in developing rat hippocampus after status epilepticus. Epilepsia 46(Suppl 5):113–117. doi:10.1111/j.1528-1167.2005.01006.x

20. Fabene PF, Navarro Mora G, Martinello M, Rossi B, Merigo F, Ottoboni L, Bach S, Angiari S, Benati D, Chakir A, Zanetti L, Schio F, Osculati A, Marzola P, Nicolato E, Homeister JW, Xia L, Lowe JB, McEver RP, Osculati F, Sbarbati A, Butcher EC, Constantin G (2008) A role for leukocyte-endothelial adhesion mechanisms in epilepsy. Nat Med 14:1377–1383. doi:10.1038/nm.1878
21. Guyon A, Nahon JL (2007) Multiple actions of the chemokine stromal cell-derived factor-1alpha on neuronal activity. J Mol Endocrinol 38:365–376. doi:10.1677/JME-06-0013
22. Lauro C, Di Angelantonio S, Cipriani R, Sobrero F, Antonilli L, Brusadin V, Ragozzino D, Limatola C (2008) Activity of adenosine receptors type 1 is required for CX3CL1-mediated neuroprotection and neuromodulation in hippocampal neurons. J Immunol 180:7590–7596. doi:10.4049/jimmunol.180.11.7590
23. Rainey-Barger EK, Rumble JM, Lalor SJ, Esen N, Segal BM, Irani DN (2011) The lymphoid chemokine, CXCL13, is dispensable for the initial recruitment of B cells to the acutely inflamed central nervous system. Brain Behav Immun 25:922–931. doi:10.1016/j.bbi.2010.10.002
24. Alvarez E, Piccio L, Mikesell RJ, Klawiter EC, Parks BJ, Naismith RT, Cross AH (2013) CXCL13 is a biomarker of inflammation in multiple sclerosis, neuromyelitis optica, and other neurological conditions. Mult Scler 19:1204–1208. doi:10.1177/1352458512473362
25. Hytönen J, Kortela E, Waris M, Puustinen J, Salo J, Oksi J (2014) CXCL13 and neopterin concentrations in cerebrospinal fluid of patients with Lyme neuroborreliosis and other diseases that cause neuroinflammation. J Neuroinflammation 11:103. doi:10.1186/1742-2094-11-103
26. Leypoldt F, Höftberger R, Titulaer MJ, Armangue T, Gresa-Arribas N, Jahn H, Rostásy K, Schlumberger W, Meyer T, Wandinger KP, Rosenfeld MR, Graus F, Dalmau J (2015) Investigations on CXCL13 in anti-N-methyl-D-aspartate receptor encephalitis: a potential biomarker of treatment response. JAMA Neurol 72:180–186. doi:10.1001/jamaneurol.2014.2956.
27. Mothapo KM, Verbeek MM, van der Velden LB, Ang CW, Koopmans PP, van der Ven A, Stelma F (2015) Has CXCL13 an added value in diagnosis of neurosyphilis?. J Clin Microbiol 53:1693–1696. doi:10.1128/JCM.02917-14
28. Kowarik MC, Cepok S, Sellner J, Grummel V, Weber MS, Korn T, Berthele A, Hemmer B (2012) CXCL13 is the major determinant for B cell recruitment to the CSF during neuroinflammation. J Neuroinflammation 9:93. doi:10.1186/1742-2094-9-93
29. Kizil C, Dudczig S, Kyritsis N, Machate A, Blaesche J, Kroehne V, Brand M (2012) The chemokine receptor cxcr5 regulates the regenerative neurogenesis response in the adult zebrafish brain. Neural Dev 7:27. doi:10.1186/1749-8104-7-27.
30. Stuart MJ, Corrigan F, Baune BT (2014) Knockout of CXCR5 increases the population of immature neural cells and decreases proliferation in the hippocampal dentate gyrus. J Neuroinflammation 11:31. doi:10.1186/1742-2094-11-31